



The novel endolysin XZ.700 effectively treats MRSA biofilms in two biofilm models without showing toxicity on human bone cells *in vitro*

Jesse W. P Kuiper , Jolanda M. A Hogervorst , Bjorn L. Herpers , Astrid D. Bakker , Jenneke Klein-Nulend , Peter A. Nolte & Bastiaan P. Krom

To cite this article: Jesse W. P Kuiper , Jolanda M. A Hogervorst , Bjorn L. Herpers , Astrid D. Bakker , Jenneke Klein-Nulend , Peter A. Nolte & Bastiaan P. Krom (2021): The novel endolysin XZ.700 effectively treats MRSA biofilms in two biofilm models without showing toxicity on human bone cells *in vitro* , Biofouling, DOI: [10.1080/08927014.2021.1887151](https://doi.org/10.1080/08927014.2021.1887151)

To link to this article: <https://doi.org/10.1080/08927014.2021.1887151>



© 2021 The Author(s). Published by Informa UK Limited, trading as Taylor & Francis Group.



[View supplementary material](#)



Published online: 21 Feb 2021.



[Submit your article to this journal](#)



[View related articles](#)



[View Crossmark data](#)

The novel endolysin XZ.700 effectively treats MRSA biofilms in two biofilm models without showing toxicity on human bone cells *in vitro*

Jesse W. P. Kuiper^a , Jolanda M. A. Hogervorst^b, Bjorn L. Herpers^c , Astrid D. Bakker^b ,
Jenneke Klein-Nulend^b , Peter A. Nolte^{a,1}  and Bastiaan P. Krom^{d,1} 

^aDepartment of Orthopedic Surgery, Spaarne Gasthuis, Hoofddorp, The Netherlands; ^bDepartment of Oral Cell Biology, Academic Centre for Dentistry Amsterdam (ACTA), University of Amsterdam and Vrije Universiteit Amsterdam, Amsterdam Movement Sciences, Amsterdam, The Netherlands; ^cDepartment of Medical Microbiology, Spaarne Gasthuis, Hoofddorp, The Netherlands; ^dDepartment of Preventive Dentistry, Academic Centre for Dentistry Amsterdam (ACTA), University of Amsterdam and Vrije Universiteit Amsterdam, Amsterdam, The Netherlands

ABSTRACT

In this *in vitro* study the effect of XZ.700, a new endolysin, on methicillin resistant *Staphylococcus aureus* (MRSA) biofilms grown on titanium was evaluated. Biofilms of *S. aureus* USA300 were grown statically and under flow, and treatment with XZ.700 was compared with povidone-iodine (PVP-I) and gentamicin. To evaluate the cytotoxic effects of XZ.700 and derived biofilm lysates, human osteocyte-like cells were exposed to biofilm supernatants, and metabolism and proliferation were quantified. XZ.700 showed a significant, concentration dependent reduction in biofilm viability, compared with carrier controls. Metabolism and proliferation of human osteocyte-like cells were not affected by XZ.700 or lysates, unlike PVP-I and gentamicin lysates which significantly inhibited proliferation. Using time-lapse microscopy, rapid biofilm killing and removal was observed for XZ.700. In comparison, PVP-I and gentamicin showed slower biofilm killing, with no apparent biofilm removal. In conclusion, XZ.700 reduced MRSA biofilms, especially under flow condition, without toxicity for surrounding bone cells.

ARTICLE HISTORY

Received 27 September 2020
Accepted 30 January 2021

KEYWORDS

Orthopaedic implant
biofilm-associated infection;
MRSA; endolysin;
cytotoxicity

Introduction

Periprosthetic joint infection and other biofilm-associated infections, such as infections of mechanical heart valves, vascular endoprostheses and pacemakers, are major complications after surgery, burdening the patient and the hospital with prolonged intravenous antibiotic treatment and multiple surgical procedures (Bozic 2005; Osmon et al. 2013; Rietbergen et al. 2016). The costs of such infections put a strain on the health care system (Brochin et al. 2018). Most of these infections are caused by *Staphylococcus* spp, with *Staphylococcus aureus* being a prominent species (Malhas et al. 2015). *S. aureus* is known to extensively form biofilms, i.e. structured microbial communities embedded in a matrix of polymeric substances (Archer et al. 2011). Bacteria within biofilms are protected against antimicrobial therapy and the host immune system; biofilm formation causes treatment

resistance and enhances the development of antibiotic resistant strains (Ricciardi et al. 2018). Surgical therapy for periprosthetic joint infection is focused on macroscopic removal of infected tissue and biofilm, i.e. (partial) exchange of arthroplasty components, rigorous tissue removal, and extensive irrigation with saline. Local antimicrobial therapy, such as irrigation with antibiotics or povidone-iodine (PVP-I) or implantation of antibiotic-releasing material can be used in addition to surgical removal, but currently, no local therapy exists that has been proven sufficiently effective to be implemented in clinical guidelines (Kuiper et al. 2013; Ruder and Springer 2017; Argenson et al. 2019).

With the worldwide rise of antibiotic-resistant microorganisms, recent studies have focused on alternative treatment modalities, that are less prone to resistance, such as light therapy, bacteriophages, and endolysins (Hughes and Webber 2017). Endolysins

CONTACT B.P. Krom  b.krom@acta.nl

¹Shared last authorship.

 Supplemental data for this article is available online at <https://doi.org/10.1080/08927014.2021.1887151>.

© 2021 The Author(s). Published by Informa UK Limited, trading as Taylor & Francis Group.

This is an Open Access article distributed under the terms of the Creative Commons Attribution-NonCommercial-NoDerivatives License (<http://creativecommons.org/licenses/by-nc-nd/4.0/>), which permits non-commercial re-use, distribution, and reproduction in any medium, provided the original work is properly cited, and is not altered, transformed, or built upon in any way.

are cell wall hydrolyzing enzymes that are produced by bacteriophages, and cause cell death to specific bacterial species, while other species are not killed (Nelson et al. 2012; Gutiérrez et al. 2018). Their use in fighting biofilm-associated infections is promising, as several endolysins have been shown to significantly reduce numbers of *S. aureus* in biofilms *in vitro* (Chopra et al. 2015; Schuch et al. 2017; Zhou et al. 2017; Olsen et al. 2018; Cha et al. 2019).

XZ.700 is a chimeric endolysin built combining parts of *S. aureus* bacteriophage endolysin Ply2638 (Abaev et al. 2013) and Lysostaphin (Sabala et al. 2014). The enzymatic cleavage of the staphylococcal cell wall by XZ.700 is dependent on both the recognition of the cell wall by a cell wall-binding domain (with SH3b homology), and by the specific hydrolytic activity of the two enzymatically active domains (an amidase and an endopeptidase). XZ.700 is produced as a recombinant protein in a microbial expression system.

The current study was designed to study the efficacy and safety of XZ.700 endolysin against *S. aureus* biofilms *in vitro*. *S. aureus* biofilms were grown on titanium discs *in vitro* in the previously described Amsterdam Active Attachment (AAA) biofilm model (static model) (Exterkate et al. 2010; Krom and Willems 2016). The effectiveness of XZ.700 endolysin was determined by the reduction in colony forming units (CFU ml⁻¹) following several treatment strategies (e.g. dose-response and time-response), compared with standard of care treatments (povidone-iodine and gentamicin). To assess whether breaking extracellular DNA bonds in the biofilm would enhance the effect of XZ.700, the combined effect with DNase I was tested. In addition, a microfluidics-based biofilm model (flow model) was applied to mimic flow-based treatment strategies (Krom and Willems 2016). Finally, the cytotoxicity of endolysin and endolysin-treated biofilms was tested using human osteocyte-like cells.

Materials and methods

Bacterial strains and culture

Methicillin-resistant *S. aureus* (MRSA) strain USA300 (Tenover and Goering 2009) was routinely cultured at 37 °C on tryptic soy agar (TSA) plates or in tryptic soy broth (TSB). To allow visualization of *S. aureus* by microscopy in the flow model, *S. aureus* USA300 was transformed with plasmid pMV158-GFP carrying a gene for green fluorescent protein (GFP) (Nieto and Espinosa 2003; Li et al. 2011). Successful

transformants were selected and maintained on TSA plates containing 2 µg ml⁻¹ of tetracycline.

Antibiotics

Endolysin XZ.700 was supplied by Microcos (Bilthoven, The Netherlands), and diluted to a solution of 250 µg ml⁻¹ in phosphate buffered saline (PBS, containing NaCl 8 g l⁻¹, KCl 0.2 g l⁻¹, Na₂HPO₄ 1 g l⁻¹, KH₂PO₄ 0.2 g l⁻¹) with the addition of 0.1% bovine serum albumin (BSA; Sigma-Aldrich, St Louis, MO, USA). Povidone-iodine (PVP-I; AddedPharma, Oss, The Netherlands) at 0.35% (3.5 µg ml⁻¹) (Ruder and Springer 2017), and gentamicin (Sigma-Aldrich, St Louis, MO, USA) at 1000 µg ml⁻¹, comparable with the tissue concentration when using local gentamicin (Diefenbeck et al. 2006; Mandell et al. 2019), were prepared in PBS from stock solutions containing 10% PVP-I and 50 mg ml⁻¹ of gentamicin, respectively.

Static biofilm model

Biofilms were grown in half strength TSB supplemented with 0.25% (w/v) D-glucose. The inoculum was prepared by diluting an overnight culture of *S. aureus* USA300 grown in TSB 1:50 in half strength TSB containing 0.25% (w/v) D-glucose. The stainless-steel lid of the AAA-model was fitted with titanium discs (diameter 9.52 mm, thickness 1.1 mm) and sterilized by autoclaving as described previously (Exterkate et al. 2010; Krom and Willems 2016). Each well of a sterile 24 well plate was filled with 1 ml of inoculum and incubated for 8 h at 37 °C to allow for adhesion of *S. aureus* to the titanium surfaces. Subsequently the medium was refreshed once for the 24 h old biofilms and following a 16 h – 8 h – 16 h regime until 48 h biofilms were obtained. After exposure to XZ.700 and control treatment agents (PVP-I and gentamicin) for 4 h (or shorter in experiments with different exposure times), the discs were irrigated with PBS, vortexed, and sonicated twice for 50 s (1 s on, 1 s off to prevent overheating, turning the disc after the first 50 s) at 20 kHz and 40% amplitude of 130 W with a probe sonicator (Sonics Vibracell VC130, Newtown, CT, USA). The number of residual viable bacteria was determined upon serial dilution and plating on TSA. All tests were performed in triplo or quadruplo and on two separate occasions.

Flow biofilm model

Biofilms were formed under flow-conditions using the Bioflux Z1000 (Fluxion Biosciences, San Francisco, CA, USA) setup (Krom and Willems 2016). The Bioflux was inoculated with GFP-expressing *S. aureus* USA300. A biofilm was allowed to grow for 16 h under constant medium flow (medium: half strength TSB + 0.25% (w/v) glucose + $2 \mu\text{g ml}^{-1}$ of tetracycline (Sigma-Aldrich, St Louis, MO, USA); pressure: 0.4 dyne cm^{-2}). After biofilm growth, for 16 h the biofilms were exposed to XZ.700 (12.5, 25 and $50 \mu\text{g ml}^{-1}$), PVP-I 0.35% or gentamicin $1000 \mu\text{g ml}^{-1}$, supplemented with $0.5 \mu\text{l ml}^{-1}$ of propidium iodine (PI) to assess cell death. The treatment solutions were supplied at a pressure of 0.4 dyne cm^{-2} . The effect of the different agents on the biofilm in terms of decrease in green fluorescence and increase in PI fluorescence was visualized with time-lapse microscopy, taking images with a 10x objective of two selected positions per channel every 2.5 min for 4 h, using brightfield (HDIC) and fluorescence (FITC) filters acquisition. Videos showing changes in fluorescence of treated and untreated controls were constructed after addition of a timestamp and a scale bar using image analysis software (ImageJ, version 1.52, W. Rasband, National Institutes of Health, Baltimore, MD, USA). Except for image cropping, no image modification was performed.

Cytotoxicity, cell metabolic activity, and proliferation

The supernatants obtained in the static model comparing XZ.700 (12.5, 25 and $50 \mu\text{g ml}^{-1}$) with PVP-I (0.35%) and gentamicin ($1000 \mu\text{g ml}^{-1}$) were used for subsequent toxicity testing, hypothesizing that not only the agent, but also the debris of lysed cells and bacteria, including bacterial toxins, have an effect on surrounding cells *in vivo*. Briefly, human osteocyte-like cells were obtained as outgrowths from collagenase-stripped pieces (1-3 mm) of human bone, obtained as surgical waste material from elective hip or knee surgery (Ethical Review Board of the VU Medical Center, Amsterdam, The Netherlands, protocol number 2016/105). Donors were adult males and females, without metabolic bone disease. No further data about the donors are available. Cells from 5 donors were pooled to obtain more repeatable results, representative of multiple individuals. Cells were cultured up to passage 5, released by incubation with 0.25% trypsin (Gibco, Invitrogen, Waltham, MA, USA), and 0.1% ethylene-diamine-tetra-acetic acid

(Merck, Darmstadt, Germany) in PBS, and seeded at $20,000 \text{ cells cm}^{-2}$ in 48-wells plates (Greiner Bio-One, Kremsmuenster, Austria). Cells were left to adhere for 24 h in culture medium consisting of Minimum Essential Medium Alpha modification (α -MEM, Thermo Fisher Scientific, Eugene, OR, USA) supplemented with 10% HyClone FetalClone1 (FC1, Thermo Fisher Scientific) and 1% penicillin, streptomycin, and fungizone-mix (PSF; Sigma, St Louis, MO, USA). After cell attachment the cells were washed and subsequently exposed to the supernatants (50% supernatant, 50% fresh culture medium without PSF) for 48 h. Seven controls were added: 100% cell culture medium, and the six different supernatants without biofilm exposure (50% in culture medium). AlamarBlue (Thermo Fisher Scientific) was added for analysis of metabolic activity. After incubation for 48 h the fluid was analyzed using a Synergy HT[®] spectrophotometer for quantification of AlamarBlue conversion (fluorescence was read in the samples at 530 nm excitation and 590 nm emission). Subsequently, the wells were emptied, $200 \mu\text{l}$ sterile water were added, cells were lysed by freezing and thawing three times, and total cell DNA was assessed using the Cyquant Cell Proliferation Assay (Molecular Probes, Eugene, OR, USA) according to the manufacturer's instructions (fluorescence was read in the samples at 480 nm excitation and 520 nm emission with a Synergy HT[®] spectrophotometer), to evaluate cell number.

Statistical analysis

Statistical analysis was performed using IBM SPSS version 23 (IBM, Armonk, NY, USA). Analysis of variance (ANOVA) and Tukey multiple range test were used to test differences between groups. Values of $p < 0.05$ were considered statistically significant.

Results

Effect of XZ.700 on MRSA biofilms in a static model

Dose dependent effect

After biofilm development for 24 and 48 h, the biofilm-containing titanium discs were immersed in serially diluted concentrations of XZ.700 ($6.25 - 400 \mu\text{g ml}^{-1}$) and a carrier control, for 4 h. For the 24 h-old biofilms, a maximum biofilm reduction of 80-90% was obtained at concentrations between $6.25 - 50 \mu\text{g ml}^{-1}$. Higher concentrations of XZ.700 did not result in higher killing; in contrast, the remaining viability after treatment with

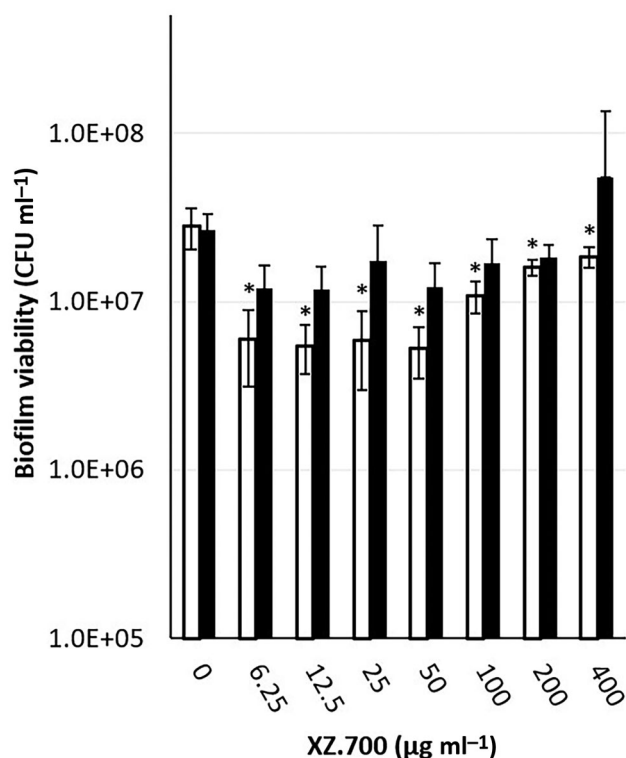


Figure 1. Dose-dependent effect of 4 h exposure to XZ.700 on the viability of 24 h (white bars) and 48 h (black bars) old MRSA biofilms. *Significant reduction in biofilm viability compared with the control, $p < 0.05$.

high concentrations was higher compared with the lower concentrations. No significant reduction was seen for the 48 h-old biofilms (Figure 1).

Comparison with povidone-iodine and gentamicin

After biofilm development for 24 and 48 h, the discs were immersed in serially diluted concentrations of XZ.700 (12.5 – 50 µg ml⁻¹), PVP-I (0.35%), gentamicin (1000 µg ml⁻¹), and a control, for 4 h. For 24 h-old biofilms, all three XZ.700 concentrations, PVP-I and gentamicin showed a significant reduction in viability, and PVP-I and gentamicin showed a higher reduction in viability than XZ.700 (95–99% vs 80–90%). For 48 h-old biofilms, all XZ.700 concentrations, PVP-I, and gentamicin showed a significant reduction in biofilm viability (Figure 2).

Effect of different exposure times and single, double, and quadruple hits

After biofilm development for 24 and 48 h, the discs were immersed in the most effective concentration of XZ.700 (25 µg ml⁻¹) for 0 (control), 15, 30, 60, 120 and 240 min. Maximum biofilm reduction was achieved after 60 min exposure and did not increase with increasing exposure times, achieving a significant reduction in viability for both 24 h and 48 h old biofilms (Figure 3A).

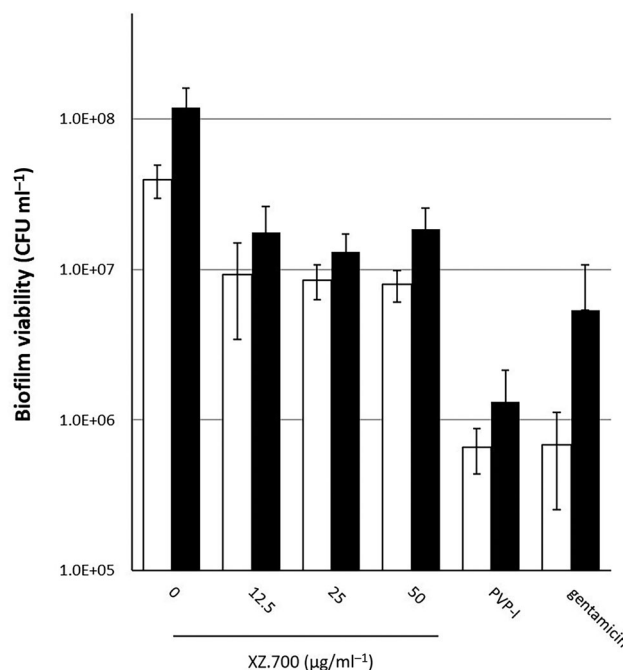


Figure 2. Comparison of the effect of 4 h exposure to XZ.700 (12.5, 25 and 50 µg ml⁻¹), PVP-I (0.35%), and gentamicin (1000 µg ml⁻¹) on biofilm viability in 24 h (white bars) and 48 h (black bars)-old MRSA biofilms. *Significant reduction in biofilm viability compared with the no treatment control, $p < 0.05$.

After biofilm development for 24 and 48 h, the titanium discs were immersed in the most effective concentration of XZ.700 (25 µg ml⁻¹) for either 120 min, 2 × 60 min or 4 × 30 min, and this was also performed with 25% of the concentration for comparison purposes, and with two controls (1 × 120 min and 4 × 30 min of PBS). For multiple hits (2 × 60 and 4 × 30 min) the medium was directly exchanged. Double or quadruple hits did not show significantly more biofilm viability reduction than single hit treatment (Figure 3B).

Effect of DNase I. After biofilm development for 24 and 48 h, the biofilm containing titanium discs were immersed in the most effective concentration of XZ.700 (25 µg ml⁻¹), DNase I (50 U ml⁻¹; with the addition of 10 mM MgCl₂, and the combination of the two. A no-treatment control (PBS + 0.1% BSA + 10 mM MgCl₂) was used as a reference. XZ.700 achieved a similar reduction in viability compared with DNase I and compared with the combined treatment methods (Figure 4).

Effect of XZ.700 on MRSA biofilms in a flow model

As shown in the supplementary videos and in Figure 5, in the Bioflux model, treatment with XZ.700 (12.5,

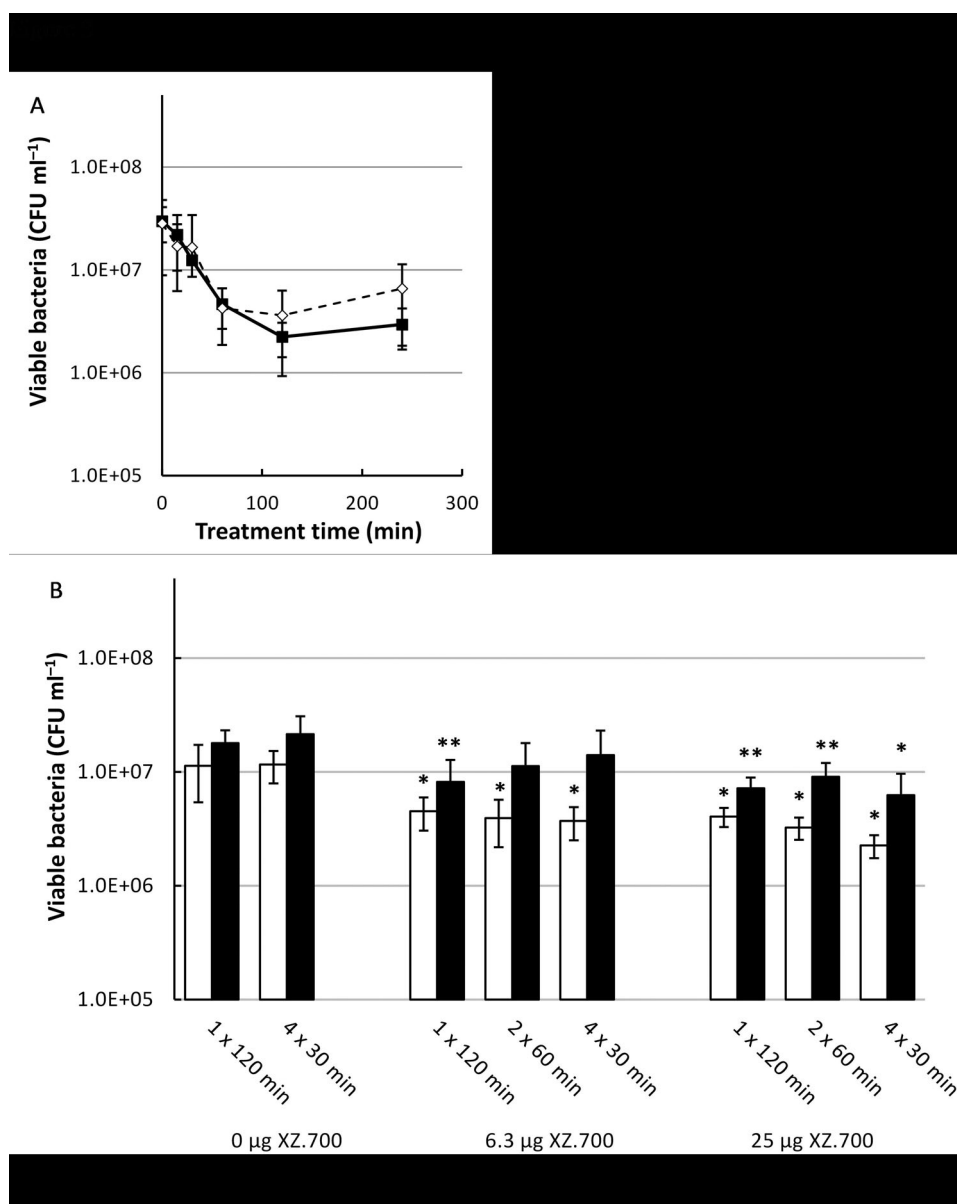


Figure 3. Panel A: Comparison of the effect of exposure times to XZ.700 ($25 \mu\text{g ml}^{-1}$) on the viability of 24 h-old (dashed line) and 48 h-old (solid line) MRSA biofilms. *Significant reduction in CFU ml^{-1} compared with the control, $p < 0.05$. Panel B: Comparison of the effect of a single hit, two hits and four hits of XZ.700 ($25 \mu\text{g ml}^{-1}$ and $6.25 \mu\text{g ml}^{-1}$) on the viability of 24 h-old (white bars) and 48 h-old (black bars) MRSA biofilms. *Significant reduction in CFU ml^{-1} compared with the respective single hit control (1 x 120 min) and four hit control (4 x 30 min), $p < 0.05$. **Significant reduction in CFU ml^{-1} compared with the four hit control (4 x 30 min), $p < 0.05$.

25 and $50 \mu\text{g ml}^{-1}$; S2, S3, S4 respectively) achieved a rapid decrease in GFP activity and visible biofilm mass, i.e. within 10 min after exposure of the biofilm to XZ.700, GFP fluorescence disappeared, a slight peak in red fluorescence was seen, and all macroscopic biofilm was gone. The control (S1) showed an increase in GFP fluorescence over the course of 4 h after a small decrease in the first minute. The biofilms exposed to PVP-I (S5) and gentamicin (S6) showed the most pronounced decrease in GFP fluorescence in the first 30 min, after which the PVP-I-exposed biofilm showed almost no

GFP activity, and the gentamicin-exposed biofilm showed some residual fluorescence. For both PVP-I and gentamicin-treated biofilms, the biomass remained visible over the course of the experiment, in contrast with the XZ.700 treated biofilms.

Cytotoxicity of XZ.700 supernatants on human bone cells

To study possible cytotoxic effects of XZ.700-induced biofilm lysates on human bone cell viability, cell

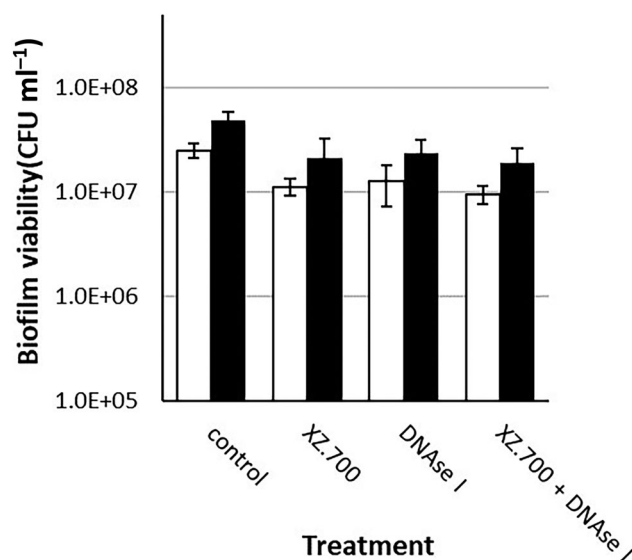


Figure 4. Comparison of the effect of 4 h exposure to XZ.700 ($25 \mu\text{g ml}^{-1}$), DNase I (50U ml^{-1}) and both combined, on the viability of 24 h-old (white bars) and 48 h-old (black bars) MRSA biofilms. *Significant reduction in biofilm viability compared with the respective no-treatment controls, $p < 0.05$.

cultures were exposed to supernatants obtained after biofilm exposure to XZ.700, PVP-I, and gentamicin.

After being exposed to the supernatants of XZ.700-treated 24 h-old biofilms (SN 24 h) and 48 h-old biofilms (SN 48 h), osteocyte-like cells showed a similar amount of DNA in comparison with untreated controls. Exposure to PVP-I (0.35%) and gentamicin ($1000 \mu\text{g ml}^{-1}$) derived lysates resulted in amounts of DNA that were significantly less (37-69%) compared with the untreated controls (Figure 6).

Using the AlamarBlue assay, exposure to all different supernatants resulted in similar, normal cell metabolism for osteocyte-like cells (all results were between 79 and 112% compared with the positive controls) (Figure 7).

Discussion

In this *in vitro* study, the new chimeric endolysin XZ.700 was effective in reducing the viability of 24 h-old and 48 h-old MRSA biofilms grown on titanium discs in a static model. In a flow model, a fast decrease in GFP fluorescence and visible biofilm mass was observed. The standard of care treatments, PVP-I and gentamicin, were used for comparison and showed a larger reduction in viability for 24 h-old biofilms in the static model, but appeared much less effective in the flow model. Furthermore, XZ.700 derived biofilm lysates showed no significant effect on metabolism and proliferation of human osteocyte-like cells, whereas PVP-I and gentamicin-derived biofilm

lysates had a large inhibitory effect on cell proliferation.

XZ.700 was tested on MRSA biofilms using a static model as well as a flow biofilm model. Generally, in the static biofilm model with titanium discs, a significant reduction in viability of 80-90% ($\sim 1 \text{ log}$) was achieved. In terms of bacterial viability count reduction, in the 24 h-old biofilm groups, PVP-I (0.35%) and high local concentrations of gentamicin ($1000 \mu\text{g ml}^{-1}$) performed better. The 48 h-old biofilm showed more treatment resistance for gentamicin, which is in line with known increased biofilm resistance to antibiotics (Mandell et al. 2019). Interestingly, this increase in resistance was not observed for XZ.700, which, like PVP-I, showed comparable reduction in biofilm viability compared with 24 h-old biofilms.

The flow biofilm model showed a rapid removal of MRSA biofilm after exposure to XZ.700, whereas PVP-I and gentamicin exposure showed decreased GFP fluorescence but no biofilm mass removal. This might be explained by the fact that in the Bioflux model, there is a continuous supply of fresh compounds and removal of cell debris that might inhibit the activity of XZ.700, representing *in vivo* conditions more closely (Díez-Aguilar et al. 2017).

In the static model, titanium was used for biofilm adherence, while in the Bioflux, for technical reasons, glass was used. Surfaces could affect the effectiveness of treatment. A study that compared biofilms formed on plastic and titanium found comparable bacterial biofilm growth for the two materials, but slower recovery after gentamicin exposure for titanium compared with plastic (Coraça-Huber et al. 2012). It should also be noted that biofilms in the Bioflux were 16 h-old biofilms, compared to 24 h-old and 48 h-old biofilms in the static model.

Another factor to be considered in the differences between static models and the clinical situation, is the large extent of biofilm formation in the static model. As discs with a surface of $\sim 150 \text{ mm}^2$ were used, a conservative estimate of the extend of biofilm formation results in at least 10^5 CFU mm^{-2} . In contrast, studies that provide information on biofilm formation (CFU mm^{-2}) on actual arthroplasty components described numbers of $\sim 10^1 \text{ CFU mm}^{-2}$ (Gómez-Barrena et al. 2012), and when determining these numbers indirectly they are $\sim 10^0$ - 10^2 (Portillo et al. 2013; Karbysheva et al. 2019). This illustrates that the clinical situation is different from the static *in vitro* model: biofilms probably grow slower, impeded by the immune system, or more bacteria may die in the

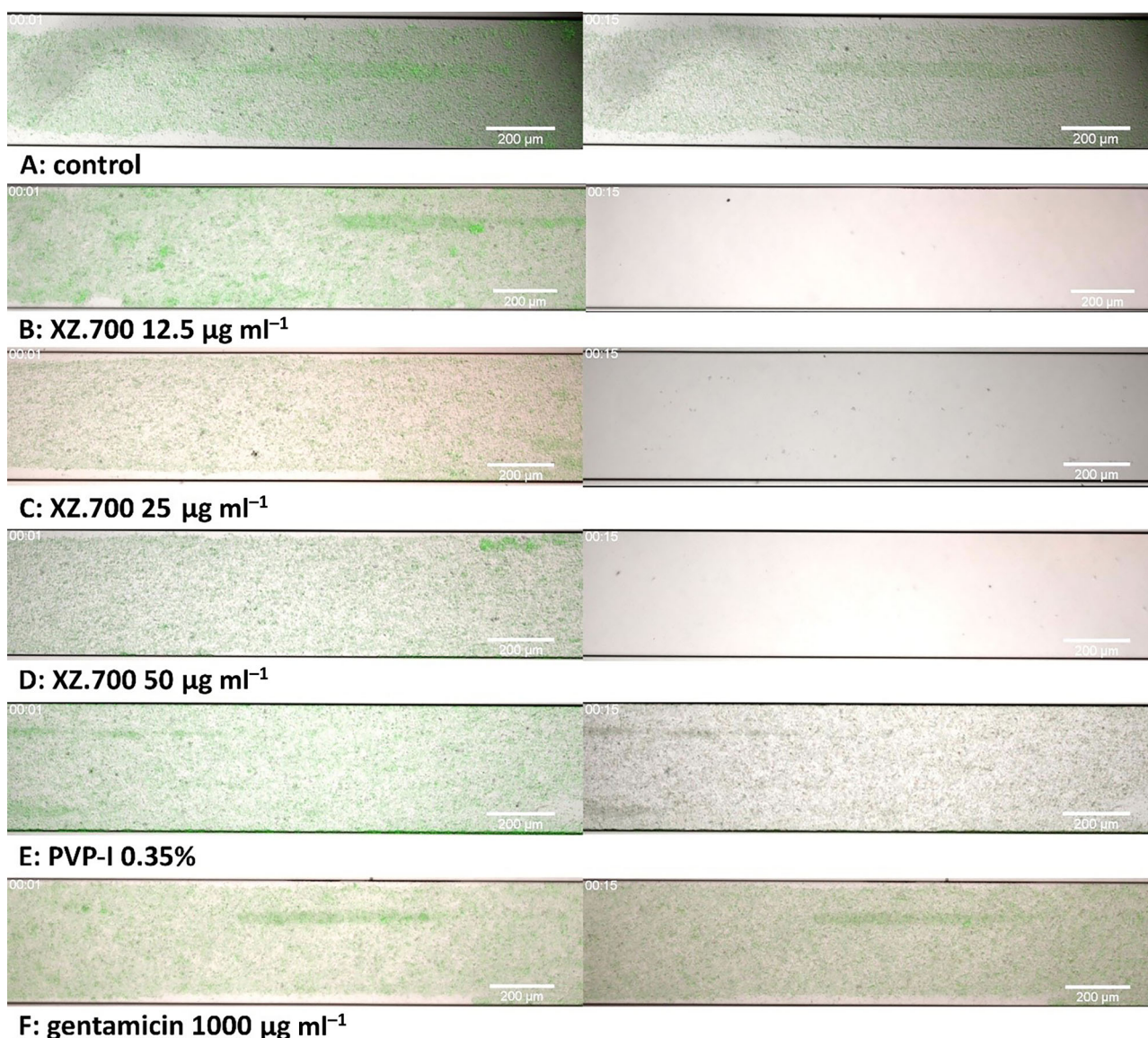


Figure 5. Time lapse microscopic images of the effect of different treatments on 16 h-old MRSA biofilms cultured under flow conditions. Images obtained 1 min (left column) and 15 min (right column) after start of flow with A: control medium, B: XZ.700 $12.5 \mu\text{g ml}^{-1}$, C: XZ.700 $25 \mu\text{g ml}^{-1}$, D: XZ.700 $50 \mu\text{g ml}^{-1}$, E: PVP-I 0.35%, F: gentamicin $1000 \mu\text{g ml}^{-1}$. Green fluorescent protein (GFP) fluorescence is shown in green, propidium iodide (PI) fluorescence (indicative for cell death) is shown in red. The size bar represents 200 μm .

process, explaining the low number of viable bacteria in biofilms. More dead bacteria in the biofilm might result in decreased penetration of antimicrobial agents into the lower layers of the biofilm. Flow models may be a better representation of the clinical situation, mimicking the physiological flow of synovial fluid in joints, i.e. removing debris and constantly supplying nutrients, but *in vivo* studies are even more essential.

Interestingly, higher endolysin concentrations and longer exposure showed a trend in less efficacy in the static model. Two possible explanations can be offered: high concentrations might evoke competitive inhibition between binding and cutting sites of the

endolysin through occupation of the bacterial surface, and longer exposure to the agent might provide new nutrients (of killed micro-organisms) to still living bacteria and thus initiate regrowth. In the flow model, the highest concentrations were not tested, but regrowth was not seen after XZ.700 treatment. This is not unexpected, as cell debris (including nutrients) are flushed away during flow.

It was hypothesized that the extracellular matrix of the biofilm could inhibit the activity of XZ.700, and DNase I treatment to disperse biofilm matrix would then enhance the effectiveness of XZ.700, as has been described for several antiseptic agents (Kaplan et al.

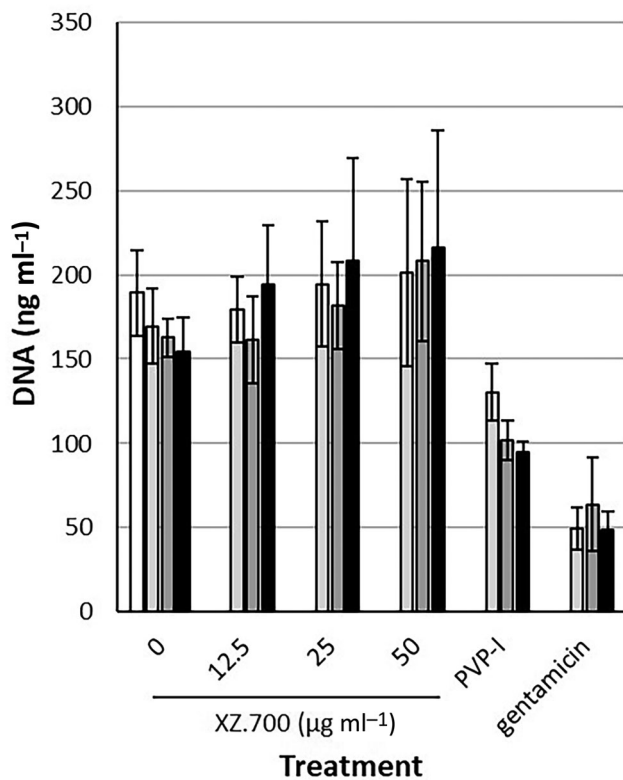


Figure 6. Proliferation of osteocyte-like cells (as amount of DNA), after 48 h exposure to 50% a-MEM and 50% MRSA biofilm supernatant, and a control (white bar; 100% a-MEM). The supernatants used were PBS + BSA (control), XZ.700 (12.5, 25 and 50 $\mu\text{g ml}^{-1}$), PVP-I (0.35%), and gentamicin (1000 $\mu\text{g ml}^{-1}$) in three different groups: without biofilm exposure (light grey bars), supernatant obtained after treatment of 24 h-old MRSA biofilm (dark grey bars), and supernatant obtained after treatment of 48 h-old MRSA biofilm (black bars). *Significantly lower than PBS + BSA and XZ.700 at 12.5, 25 and 50 $\mu\text{g ml}^{-1}$ within own group.

2012). However, as no synergistic effect between DNase I and XZ.700 was found, it may be concluded that extracellular DNA (and associated biofilm matrix components) did not limit penetration or activity of XZ.700 in biofilms *in vitro*.

The endolysin XZ.700 and the obtained supernatant did not significantly affect osteocyte-like cells *in vitro*, even after exposure for 48 h, including bacterial lysis products after biofilm treatment (supernatants).

PVP-I and gentamicin showed significantly lower yields of DNA for osteocyte-like cells. PVP-I is known to be cytotoxic, and a recent study described a safe threshold of 80 ng ml^{-1} (Zhao et al. 2016), which is 2,000 times less than the concentration of 0.35% that is used in the clinical setting (and in this study), based on another study (Ruder and Springer 2017). To test the antimicrobial effect, Zhao et al. (2016) used 0.5% PVP-I for bone matrix sterilization, and

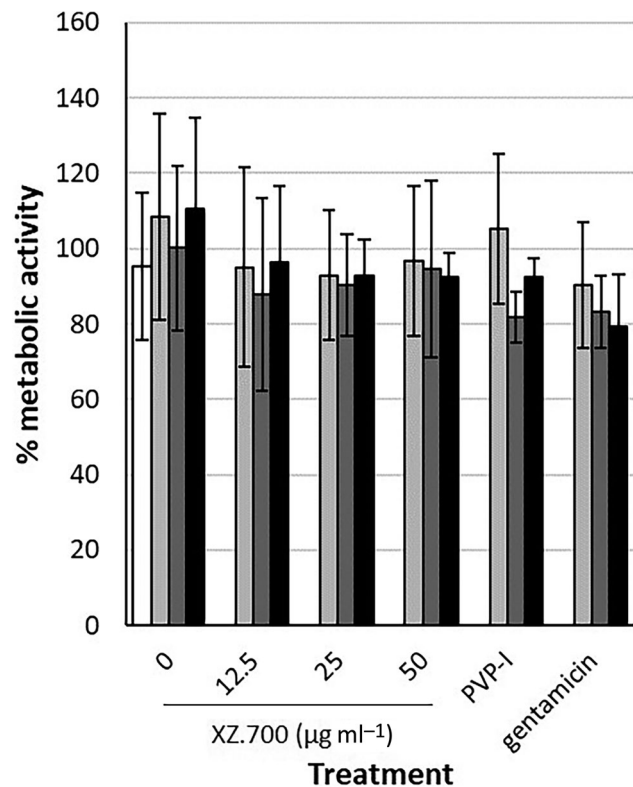


Figure 7. Metabolic activity of osteocyte-like cells, measured in percentage metabolized AlamarBlue, after 48 h exposure to 9% AlamarBlue, 45.5% a-MEM and 45.5% supernatant, and a control (white bar; 9% AlamarBlue, 91% a-MEM). The supernatants used were PBS + BSA (control), XZ.700 (12.5, 25 and 50 $\mu\text{g ml}^{-1}$), PVP-I (0.35%), and gentamicin (1000 $\mu\text{g ml}^{-1}$) in three different groups: without biofilm exposure (light grey bars), supernatant obtained after treatment of 24 h-old MRSA biofilm (dark grey bars), and supernatant obtained after treatment of 48 h-old MRSA biofilm (black bars).

found 100% reduction after immersion for 24 h in PVP-I (Zhao et al. 2016).

Gentamicin is known to affect proliferation of bone cells *in vitro*: one study found a decrease in total DNA yield for high concentrations of gentamicin ($>700 \mu\text{g ml}^{-1}$) (Isefuku et al. 2003), and another study found similar effects for another aminoglycoside, tobramycin (Miclau et al. 1995). In this study, the gentamicin-treated biofilm supernatants were diluted, resulting in a gentamicin concentration of 450 $\mu\text{g ml}^{-1}$.

For the Alamarblue based metabolic activity assays, cells were exposed to the treatment supernatants for 48 h. This *in vitro* experiment might be more extreme than the *in vivo* situation, where fluids are constantly refreshed, and (toxic) waste products are removed by the host. To the authors' knowledge, this is the first study to investigate the effect of treatment supernatants after endolysin therapy on human cells. The data indicate that XZ.700 did not have a measurable

effect on proliferation (DNA content) of osteocyte-like cells, in contrast with the standard of care, PVP-I and gentamycin. Both PVP-I and gentamycin showed an inhibitory effect on osteocyte-like cells. The observation that this inhibitory effect was not apparent in the metabolic activity (Alamarblue) can be explained by a compensatory mechanism resulting in increased metabolic activity in stressed cells.

When comparing this study to others, other *in vitro* studies have shown similar or higher reduction in *S. aureus* biofilm viability in static models for different endolysins (LysK (Zhou et al. 2017; Olsen et al. 2018), LysCSA13 (Cha et al. 2019), MR-10 (Chopra et al. 2015), CF-301 (Schuch et al. 2017)), indicating that several endolysins have shown a promising effect on biofilm-associated infections. However, endolysin therapy is still in its early stages, and although other endolysins performed well in static models, only one other study used a flow model (Biostream), achieving 80% reduction in staining (Olsen et al. 2018). Furthermore, to the authors' knowledge, a comparison with current standard of care local treatment agents, such as PVP-I and gentamicin, has not been previously described.

Conclusion

This study demonstrated the efficacy of endolysin XZ.700 on 24 h-old and 48-h old MRSA biofilms on titanium in a static model, with a reduction for MRSA biofilms of 80-90%. On 16 h-old MRSA biofilms on glass in a flow model, which is a better representation of clinical conditions, XZ.700 treatment resulted in fast killing of bacteria in the biofilm and removal of all biomass. Also, XZ.700, combined with bacterial debris components, showed no adverse effect on bone cells *in vitro*, unlike commonly used therapeutics such as PVP-I and gentamicin.

After this first *in vitro* study, XZ.700 seems a promising agent against (methicillin resistant) *S. aureus* on orthopedic material. Further *in vitro* evaluation and subsequent *in vivo* testing should be performed to determine successful application as treatment in orthopedic implant-related infections.

Acknowledgements

The authors would like to thank dr R.A.M. Exterkate for his support.

Competing interests statement

BLH works as chief medical advisor for Microcos Human Health. Microcos Human Health provided the XZ.700 used in this study. No other competing interests to be declared.

ORCID

Jesse W. P. Kuiper  <http://orcid.org/0000-0002-4173-4786>
 Bjorn L. Herpers  <http://orcid.org/0000-0003-1632-8302>
 Astrid D. Bakker  <http://orcid.org/0000-0002-0280-9124>
 Jenneke Klein-Nulend  <http://orcid.org/0000-0001-7661-199X>
 Peter A. Nolte  <http://orcid.org/0000-0002-7474-2715>
 Bastiaan P. Krom  <http://orcid.org/0000-0002-1497-1161>

References

- Abaev I, Foster-Frey J, Korobova O, Shishkova N, Kiseleva N, Kopylov P, Pryamchuk S, Schmelcher M, Becker SC, Donovan DM. 2013. Staphylococcal Phage 2638A endolysin is lytic for *Staphylococcus aureus* and harbors an inter-lytic-domain secondary translational start site. *Appl Microbiol Biotechnol.* 97:3449–3456. doi:10.1007/s00253-012-4252-4
- Archer NK, Mazaitis MJ, Costerton JW, Leid JG, Powers ME, Shirtliff ME. 2011. *Staphylococcus aureus* biofilms: properties, regulation, and roles in human disease. *Virulence.* 2:445–459. doi:10.4161/viru.2.5.17724
- Argenson JN, Arndt M, Babis G, Battenberg A, Budhiparama N, Catani F, Chen F, de Beaubien B, Ebied A, Esposito S, et al. 2019. Hip and knee section, treatment, debridement and retention of implant: Proceedings of International Consensus on Orthopedic Infections. *J Arthroplasty.* 34:S399–S419. doi:10.1016/j.arth.2018.09.025
- Bozic KJ. 2005. The impact of infection after total hip arthroplasty on hospital and surgeon resource utilization. *J Bone Joint Surg Am.* 87:1746. doi:10.2106/JBJS.D.02937
- Brochin RL, Phan K, Poeran J, Zubizarreta N, Galatz LM, Moucha CS. 2018. Trends in periprosthetic hip infection and associated costs: a population-based study assessing the impact of hospital factors using national data. *J Arthroplasty.* 33:S233–S238. doi:10.1016/j.arth.2018.02.062
- Cha Y, Son B, Ryu S. 2019. Effective removal of staphylococcal biofilms on various food contact surfaces by *Staphylococcus aureus* phage endolysin LysCSA13. *Food Microbiol.* 84:103245 doi:10.1016/j.fm.2019.103245
- Chopra S, Harjai K, Chhibber S. 2015. Potential of sequential treatment with minocycline and *S. aureus* specific phage lysin in eradication of MRSA biofilms: an *in vitro* study. *Appl Microbiol Biotechnol.* 99:3201–3210. doi:10.1007/s00253-015-6460-1
- Coraça-Huber DC, Fille M, Hausdorfer J, Pfaller K, Nogler M. 2012. *Staphylococcus aureus* biofilm formation and antibiotic susceptibility tests on polystyrene and metal surfaces. *J Appl Microbiol.* 112:1235–1243. doi:10.1111/j.1365-2672.2012.05288.x
- Diefenbeck M, Mückley T, Hofmann GO. 2006. Prophylaxis and treatment of implant-related infections by local application of antibiotics. *Injury.* 37:S95–S104. doi:10.1016/j.injury.2006.04.015
- Díez-Aguilar M, Morosini MI, Köksal E, Oliver A, Ekkelenkamp M, Cantón R. 2017. Use of Calgary and microfluidic bioFlux systems to test the activity of fosfomycin and tobramycin alone and in combination against cystic fibrosis *Pseudomonas aeruginosa* biofilms. *Antimicrob Agents Chemother.* 62:9. doi:10.1128/AAC.01650-17

- Exterkate RAM, Crielaard W, Ten Cate JM. 2010. Different response to amine fluoride by streptococcus mutans and polymicrobial biofilms in a novel high-throughput active attachment model. Calderone R, Cihlar R, editors. *Caries Res.* 44:372–379. doi:10.1159/000316541
- Gómez-Barrena E, Esteban J, Medel F, Molina-Manso D, Ortiz-Pérez A, Cordero-Ampuero J, Puértolas JA. 2012. Bacterial adherence to separated modular components in joint prosthesis: a clinical study. *J Orthop Res.* 30:1634–1639. doi:10.1002/jor.22114
- Gutiérrez D, Fernández L, Rodríguez A, García P. 2018. Are phage lytic proteins the secret weapon to kill *Staphylococcus aureus*? *mBio.* 9:1–17. doi:10.1128/mBio.01923-17
- Hughes G, Webber MA. 2017. Novel approaches to the treatment of bacterial biofilm infections. *Br J Pharmacol.* 174:2237–2246. doi:10.1111/bph.13706
- Isefuku S, Joyner CJ, Simpson AHRW. 2003. Gentamicin may have an adverse effect on osteogenesis. *J Orthop Trauma.* 17:212–216.
- Kaplan JB, LoVetri K, Cardona ST, Madhyastha S, Sadovskaya I, Jabbouri S, Izano EA. 2012. Recombinant human DNase I decreases biofilm and increases antimicrobial susceptibility in staphylococci. *J Antibiot (Tokyo).* 65:73–77. doi:10.1038/ja.2011.113
- Karbysheva S, Grigoricheva L, Golnik V, Popov S, Renz N, Trampuz A. 2019. Influence of retrieved hip- and knee-prosthesis biomaterials on microbial detection by sonication. *eCM.* 37:16–22. doi:10.22203/eCM.v037a02
- Krom 2016. In vitro models for *Candida* biofilm development. Calderone R, Cihlar R, editors. *Methods Mol Biol.* 1356:95–105.
- Kuiper JWP, Brohet RM, Wassink S, van den Bekerom MPJ, Nolte PA, Vergroesen DA. 2013. Implantation of resorbable gentamicin sponges in addition to irrigation and debridement in 34 patients with infection complicating total hip arthroplasty. *Hip Int.* 23:173–180. doi:10.5301/HIP.2013.10612
- Li J, Busscher HJ, van der Mei HC, Norde W, Krom BP, Sjollem J. 2011. Analysis of the contribution of sedimentation to bacterial mass transport in a parallel plate flow chamber: part II: use of fluorescence imaging. *Colloids Surf B Biointerfaces.* 87:427–432. doi:10.1016/j.colsurfb.2011.06.002
- Malhas AM, Lawton R, Reidy M, Nathwani D, Clift BA. 2015. Causative organisms in revision total hip & knee arthroplasty for infection: Increasing multi-antibiotic resistance in coagulase-negative *Staphylococcus* and the implications for antibiotic prophylaxis. *Surgeon.* 13:250–255. doi:10.1016/j.surge.2014.04.002
- Mandell JB, Orr S, Koch J, Nourie B, Ma D, Bonar DD, Shah N, Urish KL. 2019. Large variations in clinical antibiotic activity against *Staphylococcus aureus* biofilms of periprosthetic joint infection isolates. *J Orthop Res.* 37(7):1604–1609. doi:10.1002/jor.24291
- Miclau T, Edin ML, Lester GE, Lindsey RW, Dahners LE. 1995. Bone toxicity of locally applied aminoglycosides. *J Orthop Trauma.* 9:401–406.
- Nelson DC, Schmelcher M, Rodriguez-Rubio L, Klumpp J, Pritchard DG, Dong S, Donovan DM. 2012. Endolysins as antimicrobials. *Adv Virus Res.* 83:299–365. doi:10.1016/B978-0-12-394438-2.00007-4
- Nieto C, Espinosa M. 2003. Construction of the mobilizable plasmid pMV158GFP, a derivative of pMV158 that carries the gene encoding the green fluorescent protein. *Plasmid.* 49:281–285. doi:10.1016/s0147-619x(03)00020-9
- Olsen N, Thiran E, Hasler T, Vanzielegem T, Belibasakis G, Mahillon J, Loessner M, Schmelcher M. 2018. Synergistic removal of static and dynamic *Staphylococcus aureus* biofilms by combined treatment with a bacteriophage endolysin and a polysaccharide depolymerase. *Viruses.* 10:438. doi:10.3390/v10080438
- Osmon DR, Berbari EF, Berendt AR, Lew D, Zimmerli W, Steckelberg JM, Rao N, Hanssen A, Wilson WR, Infectious Diseases Society of America 2013. Executive summary: diagnosis and management of prosthetic joint infection: clinical practice guidelines by the Infectious Diseases Society of America. *Clin Infect Dis.* 56:1–25. doi:10.1093/cid/cis966
- Portillo ME, Salvado M, Trampuz A, Plasencia V, Rodriguez-Villasante M, Sorli L, Puig L, Horcajada JP. 2013. Sonication versus vortexing of implants for diagnosis of prosthetic joint infection. *J Clin Microbiol.* 51:591–594. doi:10.1128/JCM.02482-12
- Ricciardi BF, Muthukrishnan G, Masters E, Ninomiya M, Lee CC, Schwarz EM. 2018. *Staphylococcus aureus* evasion of host immunity in the setting of prosthetic joint infection: biofilm and beyond. *Curr Rev Musculoskelet Med.* 11:389–400. doi:10.1007/s12178-018-9501-4
- Rietbergen L, Kuiper JWP, Walgrave S, Hak L, Colen S. 2016. Quality of life after staged revision for infected total hip arthroplasty: a systematic review. *Hip Int.* 26:311–318. doi:10.5301/hipint.5000416
- Ruder JA, Springer BD. 2017. Treatment of periprosthetic joint infection using antimicrobials: dilute povidone-iodine lavage. *J Bone Jt Infect.* 2:10–14. doi:10.7150/jbji.16448
- Sabala I, Jagielska E, Bardelang PT, Czapinska H, Dahms SO, Sharpe JA, James R, Than ME, Thomas NR, Bochtler M. 2014. Crystal structure of the antimicrobial peptidase lysostaphin from *Staphylococcus simulans*. *Febs J.* 281:4112–4122. doi:10.1111/febs.12929
- Schuch R, Khan BK, Raz A, Rotolo JA, Wittekind M. 2017. Bacteriophage lysin CF-301, a potent antistaphylococcal biofilm agent. *Antimicrob Agents Chemother.* 61:1–18. doi:10.1128/AAC.02666-16
- Tenover FC, Goering RV. 2009. Methicillin-resistant *Staphylococcus aureus* strain USA300: origin and epidemiology. *J Antimicrob Chemother.* 64:441–446. doi:10.1093/jac/dkp241
- Zhao Y, Hu X, Li Z, Wang F, Xia Y, Hou S, Zhong H, Zhang F, Gu N. 2016. Use of polyvinylpyrrolidone-iodine solution for sterilisation and preservation improves mechanical properties and osteogenesis of allografts. *Sci Rep.* 6:1–13. doi:10.1038/srep38669
- Zhou Y, Zhang H, Bao H, Wang X, Wang R. 2017. The lytic activity of recombinant phage lysin LysKΔamidase against staphylococcal strains associated with bovine and human infections in the Jiangsu province of China. *Res Vet Sci.* 111:113–119. doi:10.1016/j.rvsc.2017.02.011